AGU100 ADVANCING EARTH AND SPACE SCIENCE

JGR

Journal of Geophysical Research: Earth Surface

RESEARCH ARTICLE
10.1029/2017JF004508

Key Points:
- Needle ice changed peat properties resulting in greater peat erodibility
- Needle ice processes reduced overland flow velocity by 32–44% and increased roughness by 121–170%
- Needle ice significantly increased peat loss during runoff events

Supporting Information:
- Supporting Information S1

Correspondence to:
C. Li,
gycl@leeds.ac.uk;
changjia.li@hotmail.com

Citation:
Li, C., Holden, J., & Grayson, R. (2018). Effects of needle ice on peat erosion processes during overland flow events. *Journal of Geophysical Research: Earth Surface*, *123*. https://doi.org/10.1029/2017JF004508

Received 2 OCT 2017
Accepted 2 AUG 2018
Accepted article online 22 AUG 2018

Effects of Needle Ice on Peat Erosion Processes During Overland Flow Events

Changjia Li[1], Joseph Holden[1], and Richard Grayson[1]

[1]water@leeds, School of Geography, University of Leeds, Leeds, UK

Abstract Freeze-thaw processes play a role in increasing erosion potential in upland areas, but their impact on overland flow hydraulics and fluvial erosion processes are not clearly established. We provide the first quantitative analysis demonstrating that needle ice production is a primary process contributing to upland peat erosion by enhancing peat erodibility during runoff events following thaw. To quantify the effects of needle ice on peat physical properties, overland flow hydraulics, and erosion processes, physical overland flow simulation experiments were conducted on highly frost-susceptible blanket peat with and without needle ice processes. For each treatment, overland flow rates of 0.5, 1.0, and 2.0 L/min and slopes of 2.5° and 7.5° were applied. Peat erodibility, sediment concentration, and sediment yield were significantly increased in treatments subjected to needle ice processes. Median peat losses were nearly 6 times higher in peat blocks subject to needle ice processes than in peat blocks not subject to needle ice processes. Needle ice processes decreased mean overland flow velocities by 32–44% via increased hydraulic roughness and changes to surface microtopographic features, with microrills and headcut development. Needle ice processes increased the hydrodynamic force of shear stress by 55–85%. Erosion rates under needle ice processes exhibited a significant linear relationship with stream power. Our findings indicate that models of overland flow-induced peat erosion would benefit from a winter component that properly accounts for the effects of needle ice processes on peat erodibility and erosion.

1. Introduction

Upland areas commonly subject to freeze-thaw processes are widely distributed in the middle-high latitudes and high-altitude areas of the world, with 66×10^6 km^2 of global land affected by seasonal soil freezing (Kim et al., 2011). Freeze-thaw erosion has been reported globally but particularly in parts of Europe, America, and Asia (e.g., Edwards, 2013; Edwards & Burney, 1987; Ferrick & Gatto, 2005; Labadz et al., 1991; Wang et al., 2007). While numerous studies have focused on water and wind erosion processes, much less attention has been given to freeze-thaw processes that significantly affects cohesion and strength of a frost-susceptible soil and impacts soil stability on hillslopes and resistance to running water (Gatto, 2000). A thawed surface layer overlying a frozen layer is highly susceptible to severe erosion (Wischmeier & Smith, 1978). Large amounts of eroded sediment can be produced during a thaw period and subsequent heavy rainfall (Chow et al., 2000). Freeze-thaw actions strongly interact with other erosion processes such as water erosion, wind erosion, and bank erosion (Lawler, 1986, 2005), by preparing highly erodible soil materials for transport agents. Soil erosion is enhanced by freeze-thaw, with higher rates of sediment production and transport having been observed in areas subject to freeze-thaw cycles (Francis, 1990; Labadz et al., 1991; Lawler, 2005; P. Li et al., 2016). In addition, high-latitude and high-altitude regions are more likely to be affected by increases in temperature with climate change (Intergovernmental Panel on Climate Change (IPCC), 2007), leading to greater seasonal or daily soil temperature variations and more frequent freeze-thaw cycles (Groffman et al., 2011; Kværnø & Øygarden, 2006) enhancing soil degradation and downstream sedimentation.

Soil freeze-thaw cycles can cause changes in several soil physical properties that play important roles in affecting soil resistance to water erosion such as soil cohesion, density, moisture content, critical shear stress, infiltration capacity, and soil aggregate stability (Ferrick & Gatto, 2005; Oztas & Fayetorbay, 2003; Van Klaveren & McCool, 2010). The magnitude of the effect is highly related to soil texture, cooling rate, freezing point, number, and frequency of freeze-thaw cycles and moisture content at freezing (Ferrick & Gatto, 2005; Kværnø & Øygarden, 2006; Oztas & Fayetorbay, 2003). Examples of studies conducted to study the effects of freeze-thaw cycling on soil erodibility and the erosivity of overland flow are shown in Table 1.

Table 1
Experimental Designs of Example Laboratory Soil Flume Experiments Examining the Effect of Freeze-Thaw on Runoff and Soil Erosion

References	Study area	Soil type	Freezing temperature (°C)	Needle ice production	Key findings
Edwards and Burney (1987)	Canada	loam, sandy loam, fine sandy loam	−15	NA	Soil loss ↑
Edwards and Burney (1989)	Canada	loam, sandy loam, fine sandy loam	−5	NA	Soil loss ↑
Edwards and Burney (1991)	Canada	loam, sandy loam, fine sandy loam	−5	NA	Soil loss ↑
Frame et al. (1992)	Canada	fine sandy loam	−5	NA	Soil loss ↑
Edwards et al. (1995)	Canada	fine sandy loam	−5	NA	Soil loss ↑
Van Klaveren and McCool (1998)	USA	silt loam	−22 to −12	NA	Soil erodibility ↑
Gatto (2000)	USA	clayey silt	−6 to 0	Yes	Soil cohesion ↓
Ferrick and Gatto (2005)	USA	silt	−35	NA	Sediment load ↑
Van Klaveren and McCool (2010)	USA	silt loam	−22 to −12	NA	Soil erodibility ↑
Ban et al. (2016)	China	silt loam	−25 to −15	NA	Flow velocity ↓
Liu et al. (2017)	China	silt clay loam	−12	NA	Soil detachment capacity ↑

Note. Abbreviations: ↑ = an increase; ↓ = a decrease; NA = not reported in paper.

A review of the published literature reveals that despite considerable research on soil erodibility affected by freeze-thaw cycles, the relationships between soil freeze-thaw and erosion processes have received relatively little attention. In many environments, ice segregation within soil voids is considered to be an important agent of frost weathering (Lawler, 1988a). Needle ice is an external form of ice segregation in which ice crystals grow orthogonally from a soil surface and propagate microcracks or macrocracks (Outcalt, 1971). Needle ice crystal growth gradually weakens and finally breaks up soil aggregates, while subsequent warming and thawing weakens or loosens this fractured soil, enhancing soil erodibility. Without needle ice growth, frozen soil remains resistant to water erosion, and only when the frost layer thaws does the soil at the surface become weakened (Van Klaveren & McCool, 2010). Soil needle ice growth and thawing, which affects surface soil properties, has been reported on all continents with several reports from key regions including the Andes and Rocky Mountain chains, eastern United States, northwest and central Europe, East African high mountains, New Zealand, and Japan (Lawler, 1988b). In the 30 years since Lawler's (1988b) global needle ice review and mapping study, there have been almost 500 further papers reporting the needle ice phenomenon (based on a search using Thomson Reuters Web of Science). However, few studies have been conducted to quantify erosion rates or changes to flow properties associated with needle ice and thaw (Branson et al., 1996; Lawler, 1993; Table 1).

The importance of overland flow hydraulic characteristics such as flow velocity, friction coefficients, and flow shear stress and their relationships with erosion have been widely reported (Govers et al., 2007). However, few studies have examined the hydraulic characteristics of overland flow on soils subject to needle ice processes. Ban et al. (2016) found that freeze-thaw modified overland flow velocity for a clay. Any modification of overland flow velocity has important implications as it is an important parameter for modeling soil erosion, being directly related to the soil detachment and sediment transport capacity (Holden et al., 2008).

Most studies examining soil freeze-thaw erosion processes have concentrated on mineral soils, with much less known about organic soils. Peatlands that slowly accumulate organic-rich peat (Charman, 2002), cover approximately 2.84% of the world's land area (Xu et al., 2018) and are important terrestrial carbon sinks, storing one third to half of the world's soil carbon (Yu, 2012). Of particular concern in terms of erosion are rain-fed blanket peatlands, which mainly occur on sloping ground in temperate, hyperoceanic regions with high precipitation (Gallego-Sala & Prentice, 2013) and cover 105,000 km^2 of the Earth's surface (P. Li et al., 2017). Many Northern Hemisphere blanket peatlands have experienced severe erosion and are under increasing erosion risk from future climate change (Clark et al., 2010; Gallego-Sala et al., 2010; P. Li et al., 2017), which will lead to enhanced losses of terrestrial carbon in many regions.

In many blanket peatlands with cool and wet climates, freeze-thaw processes are dominant sediment production mechanisms (Evans & Warburton, 2007; Francis, 1990; Grayson et al., 2012; Labadz et al., 1991; P. Li et al., 2016). Soil freeze-thaw processes have been evaluated through a number of laboratory and field experiments but are underrepresented in the literature for blanket peat. The physical and chemical characteristics of peat can be quite different to those of mineral soils (Hobbs, 1986). Compared to mineral soils, peat has a higher volumetric heat capacity but much lower conductivity and has significantly

Figure 1. Photographs taken at blanket peat field sites in northern England showing typical needle ice formation. Note the friable sediment layer on the upper surface of the ice mass. Also note different layers of ice needles indicating different consecutive nights of needle ice formation.

different thermal response during wetting or drying periods (FitzGibbon, 1981). This demonstrates that a strong thermal gradient can develop between a cold peat surface and warmer peat at depth (Evans & Warburton, 2007). The significant temperature gradients together with abundant moisture supply are ideal for needle ice formation (Outcalt, 1971). Due to the maritime location of many blanket peat environments, freezing is commonly diurnal and the effect of a single needle ice event can be multiplied many times through the winter season (Figure 1). The importance of needle ice formation in producing eroding peat faces has been widely reported in peatlands such as eroding upland peatlands in the United Kingdom (Legg et al., 1992; Tallis, 1973), erosion of peat remnants in Finnish Lapland (Luoto & Seppälä, 2000), and alpine mires in Lesotho (Grab & Deschamps, 2004). The growth of needle ice can lead to a *fluffy* peat surface that is loose and granular and vulnerable to being flushed off by overland flow events (Evans & Warburton, 2007), with saturation excess overland flow being a dominant flow mechanism in blanket peat systems (Holden & Burt, 2003). However, little quantitative work has been conducted on how surface roughness and overland flow are affected by needle ice formation and melting nor on quantifying how these effects impact upon peat erosion. Given the lack of quantitative data on needle ice effects on peat erosion, the aim of our study was to measure how needle ice effects soil erodibility, overland flow hydraulic characteristics and sediment production processes through a series of experiments.

2. Materials and Methods

2.1. Experimental Design

2.1.1. Sample Collection

Undisturbed bare peat blocks were carefully excavated from topsoil at Moor House National Nature Reserve (54°41′N, 2°23′W), a blanket peat site in northern England. The climate at Moor House is favorable for needle ice formation that is normally observed to grow within the upper peat layer during winter months (Evans & Warburton, 2007).

A plastic rectangular gutter (1.0-m long, 0.13-m wide, and 0.08 m in depth) was pushed parallel to the peat surface into the peat and carefully dug out to extract an undisturbed peat block. Samples were tightly sealed using plastic film to minimize peat oxidation and drying before being stored at 4 °C prior to laboratory analysis. Peat samples were extracted from peat blocks before and after subjecting the peat to needle ice processes and analyzed in the laboratory using a Morphologi G3 to capture two-dimensional images of peat particles and to calculate size and shape parameters.

2.1.2. Freezing and Thawing With Needle Ice Growth and Melting

Microhydrological and micrometeorological variables affecting needle ice growth include cooling rate, freezing point and duration, and soil moisture status (Branson et al., 1996; Outcalt, 1971). For laboratory-based experiments of needle ice growth, cooling rate is critical as it should be slow enough to simulate natural cooling, which is usually a result of radiative heat loss (Higashi & Corte, 1971;

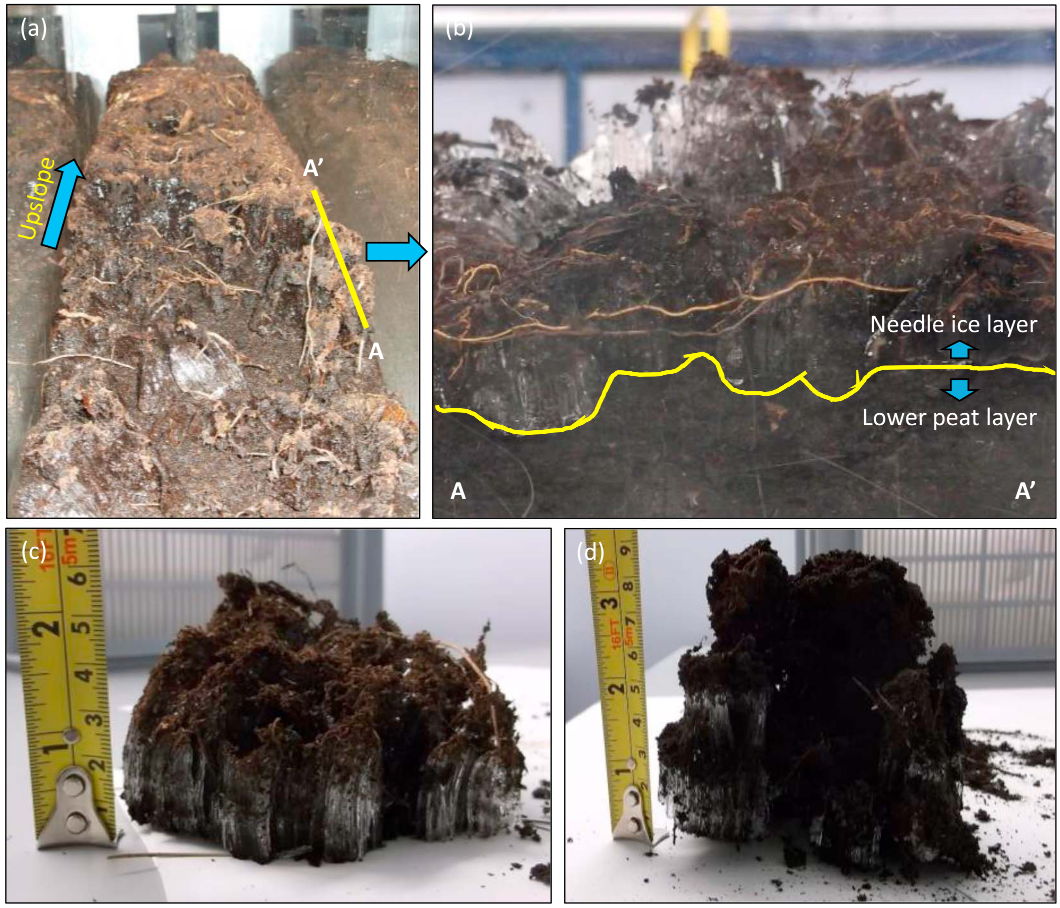

Figure 2. Morphology of laboratory needle ice growth: (a) Peat block with needle ice formation within the upper peat layers; (b) view from A-A′ cross section of the peat block. Two distinctive layers including the upper needle ice layer and the much denser undisturbed peat layer below were identified; (c and d) typical needle ice formations. Note the friable surface layer resulting from formation of needle ice on the upper surface of the ice mass.

Outcalt, 1970). However, many laboratory experiments have failed to produce radiative cooling that enhances needle ice growth and produces erodible soil (Table 1). Soil aggregate stability is negatively correlated with soil moisture content at the time of freezing (Oztas & Fayetorbay, 2003) and ice crystals grow abundantly at high moisture content, which breaks bonds holding soil particles together (Ferrick & Gatto, 2005).

To ensure that freezing would occur from the peat surface downward, the peat blocks were wrapped with heat-insulating materials on the sides and base. Peat blocks were supplied with deionized water to container capacity and then transferred from the cold store (4.0 °C) to an environmental cabinet with an initial temperature of 5.0–6.0 °C. Our preliminary tests on peat cores showed that an average cooling rate of −1.3 °C/hr contributes to ice segregation and growth. The temperature of the environmental cabinet was subsequently set to cool at 1.3 °C/hr and finally set at −1.0 °C for 5–7 days to allow continuous growth of needle ice (Lawler, 1993). This means that the particular case we investigated was a long-duration needle ice production rather than diurnal needle ice production and thaw. Both patterns have been observed in the field (Evans & Warburton, 2007). The peat was almost saturated at the start of each freeze period, and during freezing deionized water was added periodically to provide sufficient available moisture for needle ice growth. Needle ice successfully formed within the upper layer of the peat block (Figure 2). Under freezing conditions, needle ice samples were carefully removed from the peat surface and photographed, with the needle ice length being measured using calipers. The peat blocks with needle ice formation were subsequently subjected to thawing at room temperature (20 °C) for approximately 2 days.

Structure-from-Motion photogrammetric surveying was used to obtain high-resolution topographic data sets on peat blocks with (NI) and without (Non-NI) needle ice formation and thaw. The Multiscale Model to Model Cloud Comparison (M3C2) algorithm (Lague et al., 2013) in the open source CloudCompare software was used to compute cloud-to-cloud differencing and roughness of both clouds (NI and Non-NI).

2.1.3. Overland Flow Experiments

Peat blocks were placed inside soil flumes with an area of 0.13 m^2 (1.0 m in length and 0.13 m in width). Any gaps between the edge of the peat block and the soil flume were filled with plastic sheets in order to prevent leakage and enable all overland flow from the peat block to be collected. A pump and water distributor were used to supply uniform and steady water flow at a controlled and constant flow along the full flume width. Water was supplied from municipal water with an electrical conductivity of 421 ± 1 μs/cm and a pH of 7.2 ± 0.1, to minimize the effects of water quality on the hydrological and erosion response of the peat blocks during experiments.

Bower (1960) classified the gully systems in blanket peat environments into two distinct types of dissection (*Type 1* and *Type 2*). Type 1 dissection occurs on the flatter interfluve areas where peat is usually 1.5–2.0 m in depth on slopes less than 5° (Bower, 1960). Peat gullies tend to frequently branch and intersect as an intricate dendritic network (Labadz et al., 1991). Type 2 dissection is characterized by steeper slopes (exceeding 5°), with a system of sparsely branched drainage gullies incised through the peat to bedrock and aligned nearly parallel to each other (Bower, 1960; Labadz et al., 1991). It has been suggested that the transition between Type 1 and Type 2 dissection of gully system in blanket peat environments was suggested as 5° (Bower, 1960). Therefore, slope was set at 2.5° and 7.5°, respectively to characterize the peat system firmly within each type category. For each slope, the experiments were conducted under three overland flow rates (i.e., 0.5, 1.0, and 2.0 L/min) for peat blocks subject to and not subject to needle ice processes with at least two replicates for each (supporting information, Table S1). Herein overland flow rates were selected to be appropriate to the scale of the experiments while providing sufficient range to quantify variations in peat erosion under overland flow events.

2.2. Flow and Sediment Production Measurements

During each run the time of overland flow initiation was recorded, after which each test lasted for between 10 and 30 min. The durations of the simulation experiments were determined based on the time needed for steady state overland flow and sediment concentration development: a short duration for the high inflow rate but a longer duration for the low inflow rate. Total surface flow was sampled at the flume outlet every 1 or 2 min. Overland flow volumes and rates (ml/s) for each sample were measured. Samples were left to settle for 6 hr to allow deposition of the suspended sediment. The clear supernatant was decanted, and the remaining turbid liquid was transferred to a foil container and oven-dried at 65.0 °C for 48 hr prior to weighing. The dry sediment mass (mg) was calculated, and the sediment concentration (mg/ml) was calculated as the ratio of dry sediment mass (mg) to the overland flow volume (ml). The sediment yield rate ($mg \cdot m^{-2} \cdot s^{-1}$) was defined as the ratio of dry sediment mass (mg) per unit area (m^2) per sampling duration (s).

Surface flow velocities (V_s) were measured by injecting fluorescein solution at the uppermost positions within the plots. The time required for the leading edge of fluorescein dye tracer to travel to the outlets of the plots was recorded at a resolution of 0.01 s. Overland flow velocity was calculated by dividing the distance between the injection and outlet points by the time difference between injection of fluorescein solution and arrival to the outlets. The dye-tracing method was applied at 1 min intervals with three replicates for each.

2.3. Data Analysis

For a laminar flow profile, the vertical velocity distribution is shown by a quadratic equation, with zero at the bed and a maximum for surface velocity (V_s; Katz et al., 1995). The profile mean velocity (V) was calculated using equation (1):

$$V = k\,V_s \tag{1}$$

where V is mean flow velocity (cm/s); V_s is surface flow velocity (cm/s); and k is a coefficient which is 0.33 for shallow flows on bare peat surfaces under gentle slopes (Holden et al., 2008).

10.1029/2017JF004508

The overland flow was laminar and was presumed to be uniform, and the average flow depth was calculated from

$$h = q/V = Q/(Vbt) \tag{2}$$

where h is mean flow depth for the whole plot (cm); q is the unit discharge (cm^2/s); Q is the overland flow volume during t duration (ml); and b is the width of water-crossing section (cm).

The Reynolds number Re (Reynolds, 1883) and Froude number Fr were calculated by

$$\mathrm{Re} = Vh/\upsilon \tag{3}$$

$$Fr = V/(gh)^{1/2} \tag{4}$$

where g is the acceleration due to gravity (m/s^2); and υ is the kinematical viscosity (cm^2/s).

The Darcy-Weisbach friction factor f and Manning's friction coefficient n were determined by

$$f = (8ghJ)/V^2 \tag{5}$$

$$n = \left(h^{2/3} \cdot J^{1/2}\right)/V \tag{6}$$

where J is the sine of the bed slope (m/m).

Flow shear stress τ (Pa; Foster, 1982) and stream power Ω (W/m^2; Bagnold, 1966) were calculated by

$$\tau = \rho ghJ \tag{7}$$

$$\Omega = \rho gqJ \tag{8}$$

where ρ is the density of water (kg/m^3).

In this study, peat anti scouribility capacity (AS) was defined to describe the resistance of peat to overland flow scouring and calculated as

$$AS = ft/W \tag{9}$$

where AS is the peat antiscouribility capacity (L/g); f is discharge of scouring (L/min); t is the duration of scouring (min); and W is the weight of the oven-dried peat mass (g). The higher the peat AS, the lower the peat erodibility.

Data sets were tested for normality using the Anderson-Darling normality test at the $p = 0.05$ level. Student's t test was used for testing for differences between two sets of data which were both normally distributed. The data sets that were not normally distributed were transformed and retested for normality. Mann-Whitney U tests were applied when one or both sets of response variable values were still not normally distributed. Correlation analysis and stepwise regression analysis were used to determine the relationship between overland flow hydraulics and sediment yield. All statistical tests were considered significant at $p < 0.05$.

3. Results

3.1. Soil Physical Properties

Basic chemical and physical properties of the peat blocks were determined on subsampled peat (supporting information, Table S2). Needle ice processes (NI) increased porosity and decreased peat bulk density. Results from the Morphologi G3 analysis demonstrate that peat samples subject to NI produced particles with greater average length, width, and perimeter than those not subject to needle ice processes (Non-NI; supporting information, Table S2). NIs were also found to produce less rounded particles compared with Non-NI treatments.

The median particle diameter for the NI peat samples was 5.9 μm compared to 4.4 μm for the Non-NI samples. The peat soils were 92.9% and 96.7% in the grain size range from 1 to 50 μm for the NI and Non-NI treatments, respectively. Mann-Whitney U tests showed that needle ice processes had no significant impact on peat particle size distribution ($p = 0.397$).

Structure-from-Motion measurements showed that formation of needle ice leads to a higher peat surface, with a positive median topographic change of 0.0041 m (supporting information, Figure S1). The mean roughness for the NI treatment was 0.001008, which was much greater than for the Non-NI treatment (0.000887). In addition, the standard deviation of roughness on the NI treatment (0.001071) was much greater than that for the Non-NI treatment (0.000388). These results show that needle ice growth led to a rougher peat surface.

3.2. Sediment Yield

The time for overland flow initiation from NI treatments (mean = 55.7 s, $n = 6$) was 90.7% greater than that from Non-NI blocks (mean = 29.2 s, $n = 6$). Typical overland flow and sediment concentration trends for the treatments are shown in Figure 3. Overland flow rates first increased with time since overland flow generation and then attained quasi steady state values (Figure 3). For a given slope and overland flow rate, statistical analysis showed no significant difference ($p > 0.05$) in the mean or median overland flow rate between the NI and Non-NI treatments.

For the NI treatments, sediment concentrations typically peaked during the initial stage of overland flow generation before gradually decreasing to an almost constant value (Figure 3) indicating that peat erosion primarily occurred during the early stage of overland flow generation. In contrast, for the Non-NI treatments, the sediment concentration was almost constant with little variation with overland flow generation. Mann-Whitney *U* test showed that the peak sediment concentration on Non-NI treatments was significantly lower ($p = 0.020$) than that observed on NI treatments.

The mean sediment concentration (supporting information, Table S3) for the NI treatment was significantly higher than that of the Non-NI treatment (Mann-Whitney *U* test, $p = 0.013$). Needle ice processes contributed significantly to an increase in sediment concentration, particularly at steeper slopes (7.5°; Table 2). Dimensionless NI/Non-NI ratios of sediment concentration are greater than 1.0 (Figure 4a), indicating a primary effect of the needle ice processes on peat erosion. Much larger NI/Non-NI ratios of sediment concentration were found at the highest overland flow rate (2.0 L/min).

Peat losses from both the NI and Non-NI treatments were greater for the steeper flume slope and for the highest input flow rate (supporting information, Table S3). Sediment yield ratios ranged from 1.2 to 7.7 for the 0.5 and 1.0 L/min overland flow rates and up to 15.0 for the 2.0 L/min overland flow rate. The effect of needle ice processes on sediment yield was greater under the 7.5° than the 2.5° slope (Table 2 and Figure 4b).

The Non-NI treatment produced a higher peat antiscouribility capacity (supporting information, Table S3) suggesting that needle ice processes reduce peat erodibility during overland flow events. On average, needle ice processes contributed to −50.4% and −60.5% of median peat antiscouribility capacity under the 2.5° and 7.5° conditions, respectively (Table 2). Dimensionless NI/Non-NI ratios of peat antiscouribility capacity were lower than 1.0, showing a primary effect of the needle ice processes on reducing peat erodibility. Peat antiscouribility capacity ratios generally decreased with an increase in overland flow rate, with the median value declining from 0.54 at the 2.0 L/min to 0.49 at 1.5 L/min and to 0.30 at 0.5 L/min.

3.3. Overland Flow Hydraulics

For both the NI and Non-NI treatments overland flow velocities increased with increasing slope and upslope inflow rates (Table 3). Needle ice processes reduced overland flow velocity on average by 44% and 32% under the 2.5° and 7.5° conditions, respectively (Figure 5a). The effect of needle ice processes on reducing overland flow velocity was lower under the higher inflow rate and larger slope gradient. Needle ice processes increased flow depth by 85% and 55% under the 2.5° and 7.5° conditions, respectively (Figure 5b).

Overland flows were observed to be laminar with the Reynolds number (*Re*) less than 300 (Table 3) and subcritical ($Fr < 1$). The Darcy-Weisbach friction factor *f* and Manning's *n* friction coefficients were higher for NI treatments than Non-NI treatments. The NI treatments produced *f* values ranging from 5.0 to 14.4 with a median of 9.3 under the 2.5° conditions, and from 3.7 to 11.3 with a median of 8.2 under the 7.5° conditions. The median values were much lower than those of Non-NI treatments, at 29.7 and 81.1 for 2.5° and 7.5° slopes, respectively. Similarly, NI treatments produced a greater (121–170%) Manning's friction factor (*n*; Figure 5d). The higher *f* and *n* for NI treatments indicates a limited entrainment and transport capacity of

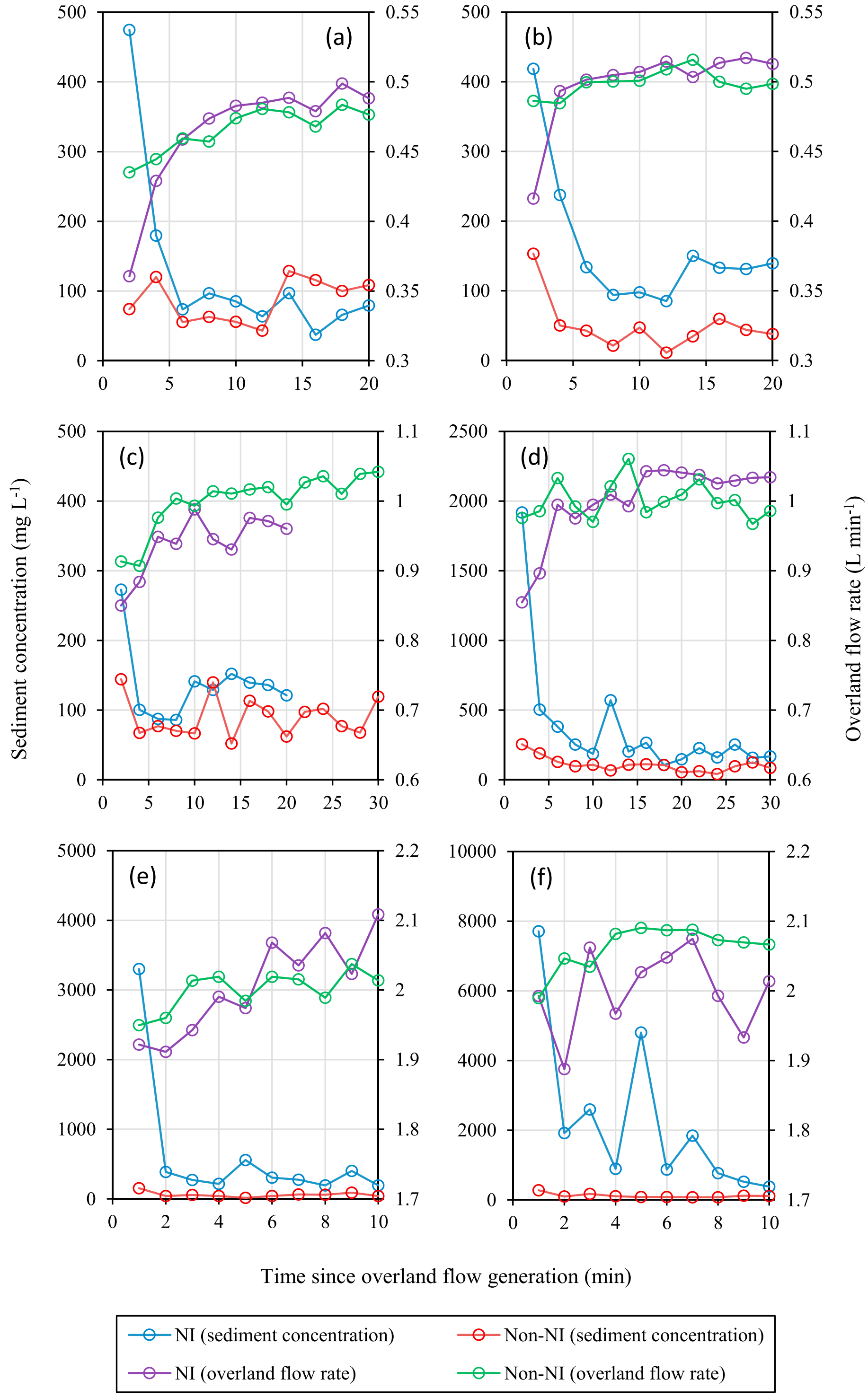

Figure 3. Overland flow and sediment concentration for representative NI and Non-NI treatments under different slopes and upslope inflow rates conditions: (a) 0.5 L/min, 2.5°; (b) 0.5 L/min, 7.5°; (c) 1.0 L/min, 2.5°; (d) 1.0 L/min, 7.5°; (e) 2.0 L/min, 2.5°; (f) 2.0 L/min, 7.5°. NI = those subject to needle ice processes; (Non-NI) = those not subject to needle ice processes.

the overland flow. The overland flow shear stress (τ) for the NI treatment was greater than that of the Non-NI treatment (Table 3), and needle ice processes increased τ by 55–85%. A similar overland flow stream power (Ω) was found for the NI and Non-NI treatments (Table 3).

Table 2
The Effects of Needle Ice Processes on Sediment Concentration, Sediment Yield and Peat Antiscouribility Capacity Under Different Slopes and Scouring Rates

Slopes	Designed flow rate (L/min)	*SC* (mg/L) In rate	*SC* (mg/L) In percentage (%)	*SY* (mg·m^{-2}·min^{-1}) In rate	*SY* (mg·m^{-2}·min^{-1}) In percentage (%)	*AS* (L/g) In rate	*AS* (L/g) In percentage (%)
2.5°	0.5	58.4	97.5	230.4	92.5	−6.9	−30.7
	1.0	35.2	50.0	159.2	21.2	−5.7	−35.6
	2.0	800.2	1,173.3	10,929.6	774.7	−15.2	−84.9
7.5°	0.5	230.8	314.4	1,844.7	666.2	−10.8	−60.7
	1.0	670.9	366.2	6,003.1	322.3	−5.5	−66.3
	2.0	752.3	869.7	24,818.3	1,403.3	−7.7	−54.6

Note. Abbreviations: *SC* = sediment concentration (mg/L); *SY* = sediment yield rate (mg·m^{-2}·min^{-1}); *AS* = peat antiscouribility capacity (L/g). Positive values indicate an increase for the NI treatments while negative values indicate a decrease compared to the Non-NI treatments.

3.4. Relationships Between Overland Flow and Sediment

Spearman's rank correlation analysis was used to test if there was a relationship between erosion and various hydraulic parameters important for peat erosion (Figure 6). For the NI treatments, peat erosion rate was closely related to stream power (p = 0.016), overland flow rate (p = 0.023), and velocity (p = 0.023). The correlation coefficient between erosion and stream power was larger at 0.895 (Figure 6). For the Non-NI treatments, overland flow velocity had a significant role in influencing erosion (p = 0.002).

For both the NI and Non-NI treatments, sediment yield generally increased with an increase in overland flow velocity, overland flow rate, flow shear stress, and stream power (Figure 7). For the NI treatments, stepwise linear regression showed that stream power was the only factor entered that predicted erosion, according to the criteria of probability-of-F-to-enter ≤0.05. The regression equation was $SY = 949.3 \times \Omega - 2{,}795.2$, with a significant ($p$ = 0.016) coefficient of determination (R^2 = 0.800). For the Non-NI treatments, stepwise linear regression showed that overland flow velocity was a good parameter for predicating erosion, with a significant (p = 0.002) coefficient of determination (R^2 = 0.935) for the regression equation.

The relationship between cumulative sediment yield and cumulative overland flow rate could be fitted by the power function $y = ax^b$, where y (mg) is the cumulative sediment yield, x (ml) is the cumulative overland flow rate, and a and b are regression coefficients (Table 4). All fitting equations were significant ($p < 0.05$). The absolute values of a for the NI treatments was much greater than those for the Non-NI treatments. However, the b coefficients of the power functions were lower for the NI treatments compared with the Non-NI treatments. These results demonstrate that the response of sediment yield to increased overland flow rates is less sensitive for the NI treatments.

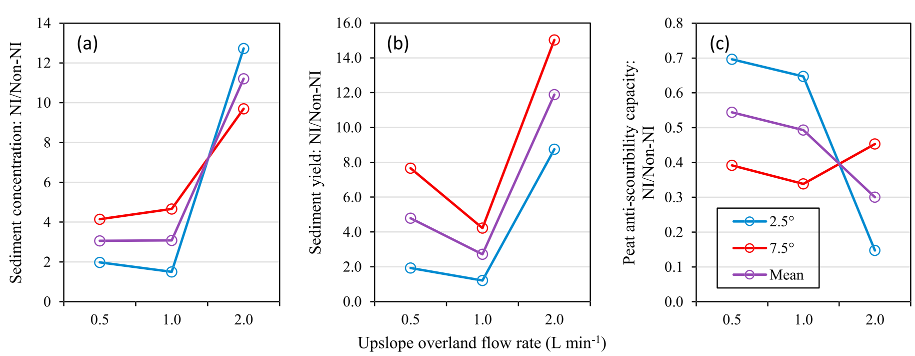

Figure 4. The ratios of NI treatment to Non-NI treatment in (a) sediment concentration; (b) sediment yield; and (c) peat anti-scouribility capacity under different slopes and scouring rates. NI = those subject to needle ice processes; (Non-NI) = those not subject to needle ice processes.

Table 3
Median Overland Flow Hydraulic Parameters for the Treatments Subject to and Not Subject to Needle Ice Processes Under Different Slopes and Scouring Rates

Slopes	Designed flow rate (L/min)	Treatment	V	h	Re	Fr	f	n	τ	Ω
2.5°	0.5	NI	4.7	4.2	62.0	0.1	62.0	35.4	1.8	2.8
		Non-NI	10.6	1.8	58.2	0.3	5.0	8.7	0.8	2.6
	1.0	NI	6.2	7.2	137.3	0.1	60.8	38.5	3.1	5.9
		Non-NI	13.2	3.7	133.6	0.3	14.4	14.2	1.6	6.0
	2.0	NI	12.7	6.2	243.1	0.2	12.7	17.1	2.6	11.0
		Non-NI	16.8	5.1	250.0	0.3	8.5	12.7	2.2	11.3
7.5°	0.5	NI	7.6	2.5	56.8	0.2	47.0	27.7	3.2	7.7
		Non-NI	12.3	1.5	58.9	0.3	9.6	11.9	2.0	7.9
	1.0	NI	13.5	3.4	138.1	0.3	24.2	20.3	4.4	18.6
		Non-NI	22.4	1.9	132.2	0.5	3.7	7.6	2.4	17.9
	2.0	NI	15.7	5.4	241.4	0.2	33.7	25.1	6.9	32.9
		Non-NI	19.0	4.3	254.5	0.3	11.3	15.3	5.5	34.4

Note. Abbreviations: V = median overland flow velocity (cm/s); h = median flow depth (mm); Re = Reynolds number; Fr = Froude number; f = Darcy-Weisbach friction factor; n = Manning's friction factor (10^{-2}); τ = flow shear stress (Pa); Ω = stream power (10^{-2} W/m^2).

4. Discussion

4.1. Effects of Needle Ice Processes on Peat Physical Properties

Needle ice processes reduced bulk density, increased porosity, and produced larger peat particles. Less rounded particles are likely to be produced from the peat surface by recent freeze thaw; however, there was no significant effect on particle size distribution. This is contrary to the results of G. Y. Li and Fan (2014), who found that freeze-thaw cycles usually increased the aggregates of small particle size groups and decreased the aggregates of the relatively larger particle size groups on a black soil in Northeast China. However, we only conducted one freeze-thaw cycle, whereas changes in soil particle size have been reported to increase with the number of freeze-thaw cycles (G. Y. Li & Fan, 2014).

For the Non-NI treatments peat erodibility was minor; continuous low erosion rates with little temporal change indicated a detachment-limited system. The overland flow velocity on the Non-NI treatments was too low to lead to continuous erosion of peat material as peat is fiber-rich and highly resistant to water erosion (Carling et al., 1997). In contrast, peat erodibility was much higher for the NI treatments despite lower overland flow velocities being observed. In line with these findings the peat antiscouribility capacity was reduced by needle ice processes. The NI treatments produced significantly higher regression coefficient *a* values compared with the Non-NI treatments (Table 4) suggesting that needle ice processes decreased the inherent resistance of peat to water erosion. Needle ice growth and thaw had strong destructive effects on peat particles. Our study is in agreement with results reported by Van Klaveren and McCool (1998) and Van Klaveren and McCool (2010) who found that erodibility for a silt loam increased after freeze-thaw. It is suggested that needle ice processes should be taken into account when analyzing peat erodibility and predicting peat erosion rate. Future work should be carried out to examine the effects of both the number and duration of needle ice processes on peat erodibility and the contribution to total erosion.

4.2. Effects of Needle Ice Processes on Overland Flow Hydraulics

Compared with the Non-NI treatments, NI treatments increased the time taken to generate overland flow due to enhanced peat infiltration capacity associated with greater porosity.

Overland flow velocity was significantly lower for NI treatments due to increased surface roughness. In addition, visual observations of the NI treatments showed that microrills and headcuts occurred and caused localized waterfalls that were responsible for lower overland flow velocities. Similar phenomena have been reported by Ban et al. (2016) who found that headcuts on thawed slopes played an important role in retarding overland flow velocity.

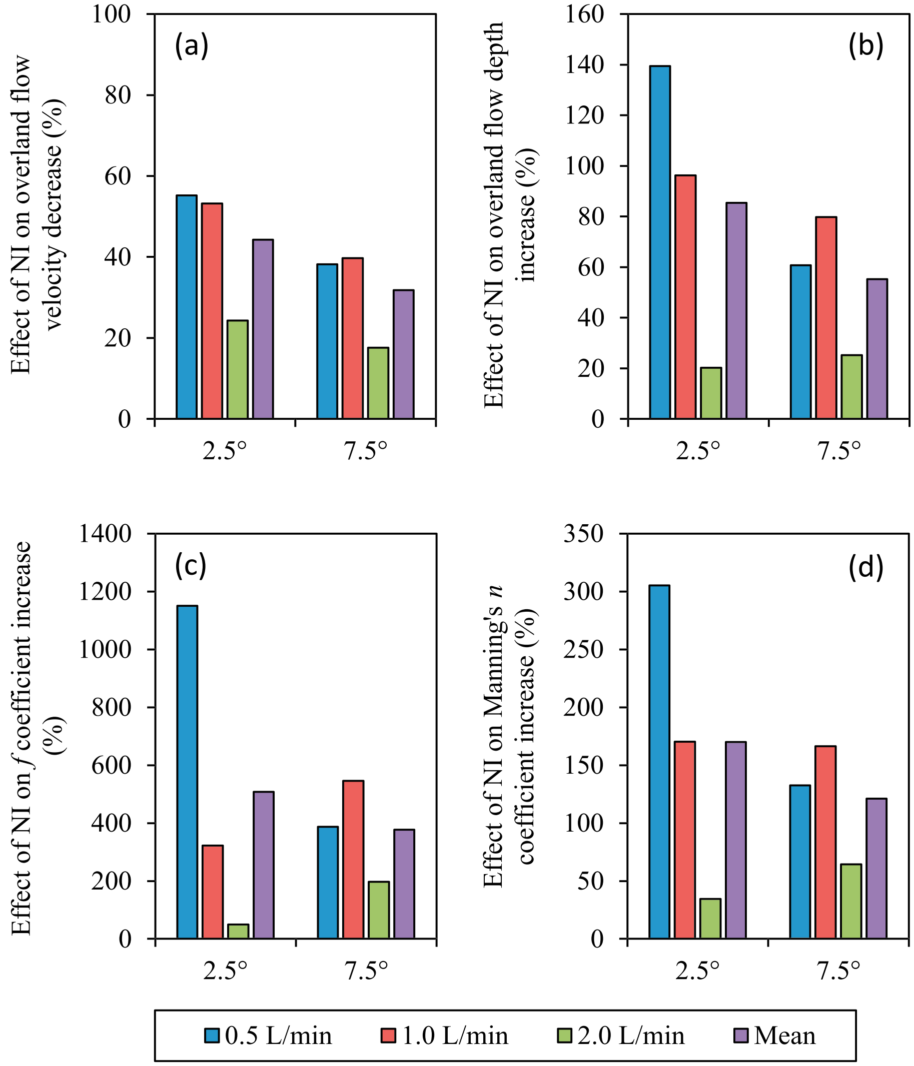

Figure 5. Effect of needle ice processes (NI) on (a) overland flow velocity decrease; (b) overland flow depth increase; (c) Darcy-Weisbach *f* friction factor increase; and (d) Manning's *n* friction factor increase under different slopes and scouring rates.

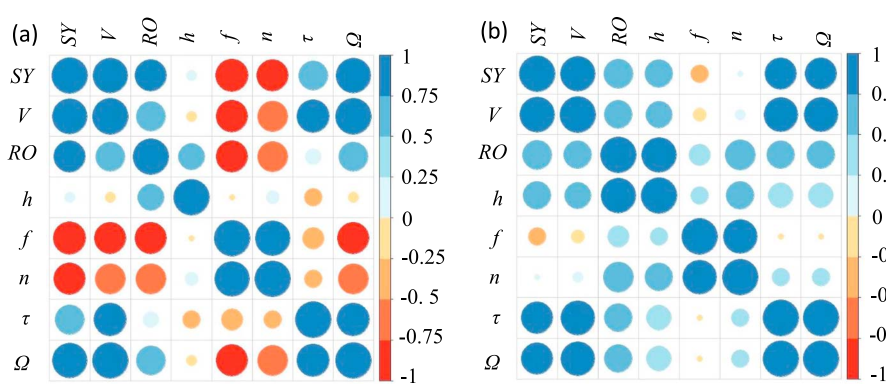

Figure 6. Correlation matrix between median peat erosion rate and different overland flow hydraulic parameters for NI (a) and Non-NI (b) treatments. Abbreviations: *SY* = sediment yield rate (mg·m^{-2}·min^{-1}); *V* = overland flow velocity (cm/s); *RO* = overland flow rate (ml/min); *h* = overland flow depth (mm); *Re* = Reynolds number; *Fr* = Froude number; *f* = Darcy-Weisbach friction factor; *n* = Manning's friction factor (10^{-2}); *τ* = flow shear stress (Pa); *Ω* = stream power (10^{-2} W/m^2).

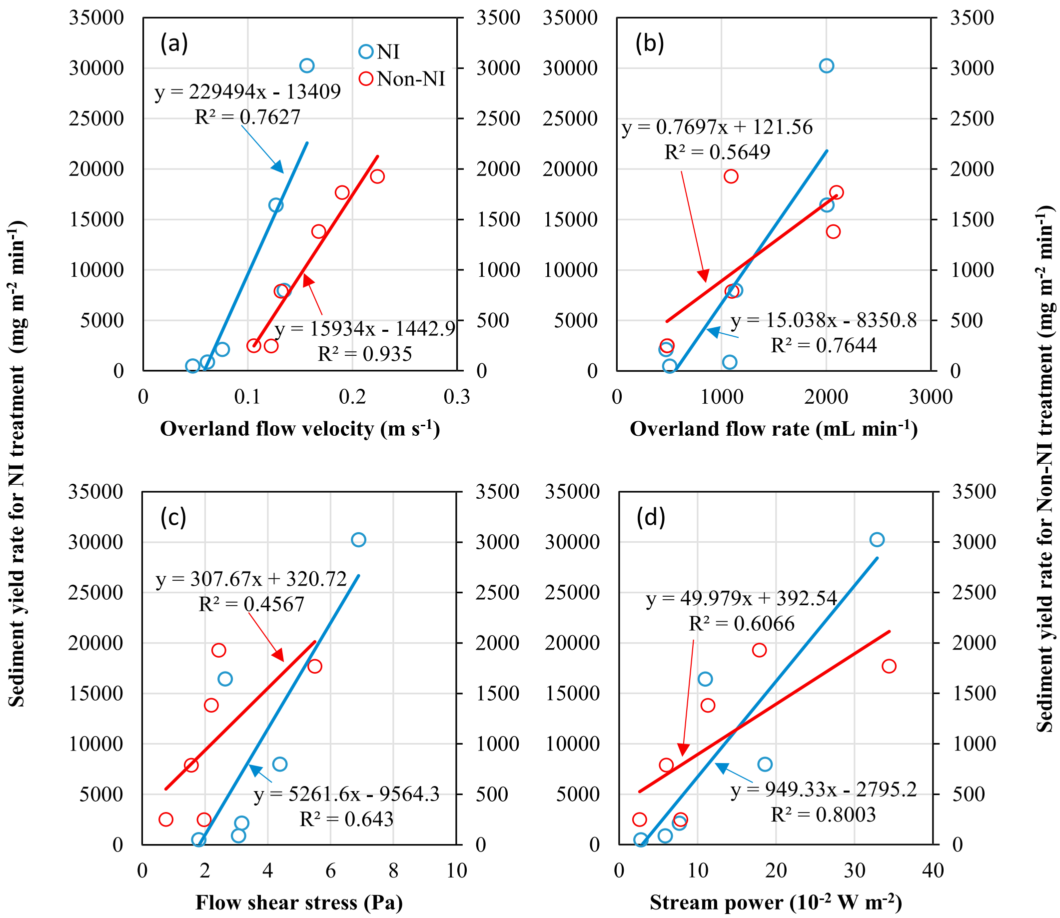

Figure 7. The relationships between mean sediment yield rate and (a) mean overland flow velocity; (b) mean overland flow rate; (c) mean flow shear stress, and (d) mean stream power for NI and Non-NI treatments.

The relative reduction in overland flow velocity caused by needle ice processes was lower under high scouring rate at 2.0 L/min than low scouring rate at 0.5 and 1.0 L/min. This results from a decrease in the ability for needle ice processes to increase hydraulic roughness under high flow rates. The effects of needle ice processes on reducing overland flow velocity and increasing overland flow depth and hydraulic roughness were found to be less on the steeper treatment.

Table 4

Regression Analysis of the Cumulative Overland Flow Rate (x) and Cumulative Sediment Yield (y) Under NI and Non-NI Treatments

Treatment	Designed flow rate (L/min)	Regression equation	*n*	R^2
NI	0.5	$y = 8.3283\ x^{0.6032}$	40	0.9983**
	1.0	$y = 235.87\ x^{0.4195}$	65	0.9810**
	2.0	$y = 260.51\ x^{0.446}$	36	0.9460**
	All	$y = 128.24\ x^{0.4672}$	141	0.7918*
Non-NI	0.5	$y = 1.7707\ x^{0.6235}$	35	0.9948**
	1.0	$y = 1.2959\ x^{0.8087}$	75	0.9724**
	2.0	$y = 10.953\ x^{0.502}$	49	0.9970**
	All	$y = 0.2414\ x^{0.9611}$	159	0.9417**

*Regression is significant at the 0.05 level. **Regression is significant at the 0.01 level.

4.3. Effects of Needle Ice Processes on Erosion Processes

The NI treatments produced similar overland flow rates to Non-NI treatments but significantly greater sediment yields. The observed difference in erosion primarily resulted from the effects of needle ice processes which increased sediment concentration, sediment yield, and reduced peat anti-scouribility capacity. This behavior has been reported for other soil types (e.g., Ferrick & Gatto, 2005; Van Klaveren & McCool, 1998; Wischmeier & Smith, 1978).

Median peat losses from the NI treatments were nearly 6 times greater than those from the Non-NI treatments. The contribution of needle ice processes to soil loss observed in our study was significantly higher than in other flume experiments by Edwards and Burney (1987) and Frame et al. (1992) where soil losses by freeze–thaw were 90% and 24%, respectively. This difference is primarily a result of the needle ice formed in our study and the expansion reduced peat particle-to-particle bonds and increasing peat erodibility. The effect of needle ice processes on increasing peat erosion was higher at high flow rate, which is in agreement with Edwards and Burney (1987) and Ferrick and Gatto (2005) who found that the increase in soil erosion by freeze-thaw generally increased with greater overland flow.

For the NI treatment, the sediment concentration rate peaked early in the initial overland flow generation and then decreased to a final constant rate. Similar results were reported by Ferrick and Gatto (2005) who applied overland flow simulation tests with flow rates ranging from 0.4, 1.2, and 2.4 L/min on a bare silt soil following a single freeze-thaw cycle. Our observed peak probably corresponds to the period when peat aggregates subjected to needle ice processes were detached and transported by overland flow. The erosion pattern appeared to be transport-limited in the initial stage of overland flow generation as more loose sediments on the surface were available for overland flow transport as overland flow started to develop at a low rate. The peat loss rate in the steady state overland flow stage was much lower compared with the initial peak rate, despite the increase in the overland flow rate and the associated transport capacity. There are two possible reasons. First, this could be caused by exhaustion of the friable needle ice derived layer and an associated detachment-limited erosion pattern when steady state overland flow was achieved. Second, overland flow for the NI treatments was often concentrated; visual observations showed that microrills occurred. There were therefore also areas with a friable needle ice-derived peat layer but with little occurrence of overland flow, suggesting that not all friable peat materials were washed off by running water. For the Non-NI treatment, the continuous low erosion rates with little temporal change indicated a detachment-limited system, as fresh peat is fiber-rich and highly resistant to water erosion, requiring a high flow velocity before continuous erosion of peat material occurs (Carling et al., 1997).

In this study, the main blanket peat erosion processes include sediment supply by needle ice processes and sediment transport by running water. Without sediment supply processes considered, sediment transport generally increases with an increase in overland flow velocity and the associated increased detachment capacity. Our results showed that peat blocks with needle ice treatments had greater hydraulic roughness and lower flow velocity which may indicate a lower sediment transport capacity. However, significantly greater sediment was measured on peat blocks with needle ice treatments than nonneedle ice treatments. This pattern shows that overland flow with relatively lower velocity is still capable of transporting more peat materials when more peat materials are available. The results demonstrate that where needle ice processes loosen particles from the peat surface, even small amounts of surface runoff may result in large amounts of erosion.

It has been widely reported that peatland streams have positive hysteresis in the relationship between suspended sediment concentration and discharge, showing peak suspended sediment concentration occurs ahead of peak flow (Evans & Warburton, 2007). The usual explanation for the positive hysteresis is sediment exhaustion as supply of erodible peat particles by weathering processes (e.g., rainsplash, freeze-thaw, and desiccation) is important for transport by water and wind. An alternative explanation for the positive hysteresis for areas with freeze-thaw needle ice is that overland flow on peat surfaces with needle ice formation and melting is easily spatially concentrated into efficient transport flowpaths, while areas with little occurrence of overland flow still have available friable peat layer that could be transported during future flow events.

4.4. Limitations

In order to produce quantifiable results with good levels of experimental control, bounded plots with inflow simulation techniques were used in this study. The size of the peat blocks we used was fairly small but meant that it was feasible to obtain undisturbed peat blocks for careful collection, transport, and storage in the laboratory. However, it should be noted that for natural peat deposits the depth of the friable upper layer disturbed by needle ice may sometimes be 10 cm or more (Evans & Warburton, 2007), and so our experiments may underrepresent roughness effects that occur in the field, particularly where there is a much larger scale hummocky peat surface. There may also have been other effects on surface roughness if we had simulated repeated diurnal needle ice and thaw processes, and so these processes require further investigation. It should also be noted that our study used simulated upslope inflow and excluded responses to raindrop impact, while under natural rainfall conditions raindrops provide the primary force to initiate peat particle detachment (C. J. Li et al., 2018). Thus, more significant effects of needle ice processes on increasing peat erosion could be expected under combined rainfall and overland flow conditions and exploration of these processes could be undertaken in future work.

5. Conclusions

Overland flow derived peat erodibility was found to be minor for peat blocks not subject to needle ice processes. However, needle ice processes dramatically increased peat erodibility and reduced peat stability. Needle ice growth and expansion acts to detach particles from the otherwise resistant peat surface. Needle ice processes significantly reduced the surface flow velocity with the average reductions ranging from 32% to 44%, mainly through increased hydraulic roughness and changed surface microtopographic features, with microrills and headcuts developing. Needle ice treatments increased overland flow shear stress by 55–85%, compared with the treatments not subject to needle ice processes. Peat erosion rates for the needle ice treatments showed a significant linear relationship with stream power.

Peat erosion processes are determined by the combined effects of peat erodibility that is largely determined by needle ice processes and overland flow hydraulic characteristics. However, peat erosion processes can alter peat erodibility during a runoff event and can alter overland flow hydraulics by increasing suspended sediment content and changing surface roughness.

Median peat losses under needle ice treatments were nearly 6 times greater than those from treatments not subject to needle ice processes. Needle ice processes significantly increased peat erosion risk during overland flow events. This highlights that reducing bare areas of upland peat may play an important role in reducing peat erosion through protecting it from the disruptive effects of needle ice processes.

Needle ice is a primary process contributing to upland peat erosion by enhancing peat erodibility and modifying overland flow hydraulics including overland flow velocity and hydraulic roughness during runoff events that follow thaw. Models of overland flow-induced peat erosion should have a winter component that properly accounts for the effects of freeze-thaw (P. Li et al., 2016) and especially needle ice processes, in order to successfully predict hillslope erosion and sediment yield for watersheds in areas influenced by freezing and thawing.

Acknowledgments
The work was funded by the River Basin Processes and Management cluster (School of Geography, University of Leeds), the China Scholarship Council and the University of Leeds (File 201406040068). Many thanks to Damian Lawler from the Centre for Agroecology, Water and Resilience, Coventry University (UK) who provided helpful suggestions through emails about how to produce needle ice under laboratory conditions. David Ashley from the School of Geography, University of Leeds is gratefully acknowledged for his assistance in preparing the experimental materials. Susanne Patel from the School of Chemical and Process Engineering, University of Leeds kindly provided use of the Malvern Morphologi G3S. The data used are listed in the tables in the manuscript and supporting information while further data in support of this paper are available at the Research Leeds Data Repository: https://doi.org/10.5518/374 (Li et al., 2018).

References

Bagnold, R. A. (1966). *An approach to the sediment transport problem from general physics*. Washington, DC: U.S. Government Printing Office.

Ban, Y., Lei, T., Liu, Z., & Chen, C. (2016). Comparison of rill flow velocity over frozen and thawed slopes with electrolyte tracer method. *Journal of Hydrology*, *534*, 630–637. https://doi.org/10.1016/j.jhydrol.2016.01.028

Bower, M. (1960). Peat erosion in the Pennines. *Advancement of Science*, *64*, 323–331.

Branson, J., Lawler, D. M., & Glen, J. W. (1996). Sediment inclusion events during needle ice growth: A laboratory investigation of the role of soil moisture and temperature fluctuations. *Water Resources Research*, *32*(2), 459–466. https://doi.org/10.1029/95WR03400

Carling, P. A., Glaister, M. S., & Flintham, T. P. (1997). The erodibility of upland soils and the design of preafforestation drainage networks in the United Kingdom. *Hydrological Processes*, *11*(15), 1963–1980. https://doi.org/10.1002/(SICI)1099-1085(199712)11:15<1963::AID-HYP542>3.0.CO;2-M

Charman, D. (2002). *Peatlands and environmental change*. Chichester, UK: John Wiley & Sons Ltd.

Chow, T. L., Rees, H. W., & Monteith, J. (2000). Seasonal distribution of runoff and soil loss under four tillage treatments in the upper St. John River valley New Brunswick, Canada. *Canadian Journal of Soil Science*, *80*(4), 649–660. https://doi.org/10.4141/S00-006

Clark, J. M., Gallego-Sala, A. V., Allott, T. E. H., Chapman, S. J., Farewell, T., Freeman, C., et al. (2010). Assessing the vulnerability of blanket peat to climate change using an ensemble of statistical bioclimatic envelope models. *Climate Research*, *45*, 131–150. https://doi.org/10.3354/cr00929

Edwards, L. M. (2013). The effects of soil freeze—Thaw on soil aggregate breakdown and concomitant sediment flow in Prince Edward Island: A review. *Canadian Journal of Soil Science*, *93*(4), 459–472. https://doi.org/10.1139/CJSS2012-059

Edwards, L. M., Burney, J. R. (1987). Soil erosion losses under freeze/thaw and winter ground cover using a laboratory rainfall simulator. National Research Council, Division of Building Research.

Edwards, L. M., & Burney, J. R. (1989). The effect of antecedent freeze-thaw frequency on runoff and soil loss from frozen soil with and without subsoil compaction and ground cover. *Canadian Journal of Soil Science*, *69*(4), 799–811. https://doi.org/10.4141/cjss89-080

Edwards, L. M., & Burney, J. R. (1991). Sediment concentration of interrill runoff under varying soil, ground cover, soil compaction, and freezing regimes. *Journal of Environmental Quality*, *20*(2), 403–407. https://doi.org/10.2134/jeq1991.00472425002000020011x

Edwards, L. M., Burney, J. R., & Frame, P. A. (1995). Rill sediment transport on a Prince Edward Island (Canada) fine sandy loam. *Soil Technology*, *8*(2), 127–138. https://doi.org/10.1016/0933-3630(95)00009-2

Evans, M., & Warburton, J. (2007). *Geomorphology of upland peat: Erosion, form and landscape change*. Oxford, UK: John Wiley & Sons. https://doi.org/10.1002/9780470798003

Ferrick, M. G., & Gatto, L. W. (2005). Quantifying the effect of a freeze–thaw cycle on soil erosion: Laboratory experiments. *Earth Surface Processes and Landforms*, *30*(10), 1305–1326. https://doi.org/10.1002/esp.1209

FitzGibbon, J. E. (1981). Thawing of seasonally frozen ground in organic terrain in Central Saskatchewan. *Canadian Journal of Earth Sciences*, *18*(9), 1492–1496. https://doi.org/10.1139/e81-139

Foster, G. (1982). Modeling the erosion process. In C. T. Haan, H. P. Johnson, & D. L. Brakensiek (Eds.), *Hydrologic modelling of small watersheds*, *Am. Soc. Agric. Eng. Monogr* (Vol. 5, pp. 297–382).

Frame, P. A., Burney, J. R., & Edwards, L. (1992). Laboratory measurement of freeze thaw, compaction, residue and slope effects on rill erosion. *Canadian Agricultural Engineering*, *34*, 143–149.

Francis, I. (1990). Blanket peat erosion in a mid-Wales catchment during two drought years. *Earth Surface Processes and Landforms*, *15*(5), 445–456. https://doi.org/10.1002/esp.3290150507

Gallego-Sala, A. V., Clark, J. M., House, J. I., Orr, H. G., Prentice, I. C., Smith, P., et al. (2010). Bioclimatic envelope model of climate change impacts on blanket peatland distribution in Great Britain. *Climate Research*, *45*, 151–162. https://doi.org/10.3354/cr00911

Gallego-Sala, A. V., & Prentice, I. C. (2013). Blanket peat biome endangered by climate change. *Nature Climate Change*, *3*(2), 152–155. https://doi.org/10.1038/NCLIMATE1672

Gatto, L. W. (2000). Soil freeze–thaw-induced changes to a simulated rill: Potential impacts on soil erosion. *Geomorphology*, *32*(1-2), 147–160. https://doi.org/10.1016/S0169-555X(99)00092-6

Govers, G., Giménez, R., & Van Oost, K. (2007). Rill erosion: Exploring the relationship between experiments, modelling and field observations. *Earth-Science Reviews*, *84*(3-4), 87–102. https://doi.org/10.1016/j.earscirev.2007.06.001

Grab, S. W., & Deschamps, C. L. (2004). Geomorphological and geoecological controls and processes following gully development in alpine mires, Lesotho. *Arctic, Antarctic, and Alpine Research*, *36*(1), 49–58. https://doi.org/10.1657/1523-0430(2004)036[0049:GAGCAP]2.0.CO;2

Grayson, R., Holden, J., Jones, R. R., Carle, J. A., & Lloyd, A. R. (2012). Improving particulate carbon loss estimates in eroding peatlands through the use of terrestrial laser scanning. *Geomorphology*, *179*, 240–248. https://doi.org/10.1016/j.geomorph.2012.08.015

Groffman, P. M., Hardy, J. P., Fashu-Kanu, S., Driscoll, C. T., Cleavitt, N. L., Fahey, T. J., & Fisk, M. C. (2011). Snow depth, soil freezing and nitrogen cycling in a northern hardwood forest landscape. *Biogeochemistry*, *102*(1-3), 223–238. https://doi.org/10.1007/s10533-010-9436-3

Higashi, A., & Corte, A. E. (1971). Solifluction: a model experiment. *Science*, *171*(3970), 480–482. https://doi.org/10.1126/science.171.3970.480

Hobbs, N. B. (1986). Mire morphology and the properties and behaviour of some British and foreign peats. *Quarterly Journal of Engineering Geology and Hydrogeology*, *19*(1), 7–80. https://doi.org/10.1144/GSL.QJEG.1986.019.01.02

Holden, J., & Burt, T. P. (2003). Runoff production in blanket peat covered catchments. *Water Resources Research*, *39*(7), 1191. https://doi.org/10.1029/2002WR001956

Holden, J., Kirkby, M. J., Lane, S. N., G, D., Milledge, C. J., Brookes, V. H., & McDonald, A. T. (2008). Overland flow velocity and roughness properties in peatlands. *Water Resources Research*, *44*, W06415. https://doi.org/10.1029/2007WR006052

Intergovernmental Panel on Climate Change (IPCC) (2007). *Climate change 2007: The physical science basis*. Geneva: IPCC.

Katz, D. M., Watts, F. J., & Burroughs, E. R. (1995). Effects of surface roughness and rainfall impact on overland flow. *Journal of Hydraulic Engineering*, *121*(7), 546–553. https://doi.org/10.1061/(ASCE)0733-9429(1995)121:7(546)

Kim, Y., Kimball, J. S., McDonald, K. C., & Glassy, J. (2011). Developing a global data record of daily landscape freeze/thaw status using satellite passive microwave remote sensing. *IEEE Transactions on Geoscience and Remote Sensing*, *49*(3), 949–960. https://doi.org/10.1109/TGRS.2010.2070515

Kværnø, S. H., & Øygarden, L. (2006). The influence of freeze–thaw cycles and soil moisture on aggregate stability of three soils in Norway. *Catena*, *67*(3), 175–182. https://doi.org/10.1016/j.catena.2006.03.011

Labadz, J., Burt, T., & Potter, A. (1991). Sediment yield and delivery in the blanket peat moorlands of the southern Pennines. *Earth Surface Processes and Landforms*, *16*(3), 255–271. https://doi.org/10.1002/esp.3290160306

Lague, D., Brodu, N., & Leroux, J. (2013). Accurate 3D comparison of complex topography with terrestrial laser scanner: Application to the Rangitikei canyon (NZ). *ISPRS Journal of Photogrammetry and Remote Sensing*, *82*, 10–26. https://doi.org/10.1016/j.isprsjprs.2013.04.009

Lawler, D. M. (1986). River bank erosion and the influence of frost: A statistical examination. *Transactions of the Institute of British Geographers*, *11*(2), 227–242. https://doi.org/10.2307/622008

Lawler, D. M. (1988a). A bibliography of needle ice. *Cold Regions Science and Technology*, *15*(3), 295–310. https://doi.org/10.1016/0165-232X(88)90076-6

Lawler, D. M. (1988b). Environmental limits of needle ice: A global survey. *Arctic and Alpine Research*, *20*(2), 137–159. https://doi.org/10.2307/1551494

Lawler, D. M. (1993). Needle ice processes and sediment mobilization on river banks: The river Ilston, West Glamorgan, UK. *Journal of Hydraulic*, *150*(1), 81–114. https://doi.org/10.1016/0022-1694(93)90157-5

Lawler, D. M. (2005). The importance of high-resolution monitoring in erosion and deposition dynamics studies: Examples from estuarine and fluvial systems. *Geomorphology*, *64*(1-2), 1–23. https://doi.org/10.1016/j.geomorph.2004.04.005

Legg, C. J., Maltby, E., & Proctor, M. C. F. (1992). The ecology of severe moorland fire on the North York moors: Seed distribution and seedling establishment of Calluna vulgaris. *Journal of Ecology*, *80*(4), 737–752. https://doi.org/10.2307/2260863

Li, C. J., Holden, J., & Grayson, R. (2018). Effects of rainfall, overland flow and their interactions on peatland interrill erosion processes. *Earth Surface Processes and Landforms*, *43*(7), 1451–1464. https://doi.org/10.1002/esp.4328

Li, G. Y., & Fan, H. M. (2014). Effect of freeze-thaw on water stability of aggregates in a black soil of Northeast China. *Pedosphere*, *24*(2), 285–290. https://doi.org/10.1016/S1002-0160(14)60015-1

Li, P., Holden, J., Irvine, B., & Grayson, R. (2016). PESERA-PEAT: A fluvial erosion model for blanket peatlands. *Earth Surface Processes and Landforms*, *41*(14), 2058–2077. https://doi.org/10.1002/esp.3972

Li, P., Holden, J., Irvine, B., & Mu, X. (2017). Erosion of Northern Hemisphere blanket peatlands under 21st-century climate change. *Geophysical Research Letters*, *44*, 3615–3623. https://doi.org/10.1002/2017GL072590

Liu, H., Yang, Y., Zhang, K., & Sun, C. (2017). Soil erosion as affected by freeze-thaw regime and initial soil moisture content. *Soil Science Society of America Journal*, *81*(3), 459–467. https://doi.org/10.2136/sssaj2016.08.0271

Luoto, M., & Seppälä, M. (2000). Summit peats ('peat cakes') on the fells of Finnish Lapland: Continental fragments of blanket mires? *The Holocene*, *10*(2), 229–241. https://doi.org/10.1191/095968300670047420

Outcalt, S. I. (1970). A study of time dependence during serial needle ice events. *Archiv für Meteorologie, Geophysik und Bioklimatologie, Serie A*, *19*(3), 329–337. https://doi.org/10.1007/BF02250898

Outcalt, S. I. (1971). An algorithm for needle ice growth. *Water Resources Research*, *7*(2), 394–400. https://doi.org/10.1029/WR007i002p00394

Oztas, T., & Fayetorbay, F. (2003). Effect of freezing and thawing processes on soil aggregate stability. *Catena*, *52*(1), 1–8. https://doi.org/10.1016/S0341-8162(02)00177-7

Reynolds, O. (1883). An experimental investigation of the circumstances which determine whether the motion of water shall be direct or sinuous, and of the law of resistance in parallel channels. *Philosophical Transactions of the Royal Society*, *174*(0), 935–982. https://doi.org/10.1098/rstl.1883.0029

Tallis, J. H. (1973). Studies on southern Pennine peats: V. Direct observations on peat erosion and peat hydrology at featherbed Moss, Derbyshire. *Journal of Ecology*, *61*(1), 1–22. https://doi.org/10.2307/2258913

Van Klaveren, R. W., & McCool, D. K. (1998). Erodibility and critical shear of a previously frozen soil. *Transactions of ASAE*, *41*(5), 1315–1321. https://doi.org/10.13031/2013.17304

Van Klaveren, R. W., & McCool, D. K. (2010). Freeze–thaw and water tension effects on soil detachment. *Soil Science Society of America Journal*, *74*(4), 1327–1338. https://doi.org/10.2136/sssaj2009.0360

Wang, D. Y., Ma, W., Niu, Y. H., Chang, X. X., & Wen, Z. (2007). Effects of cyclic freezing and thawing on mechanical properties of Qinghai–Tibet clay. *Cold Regions Science and Technology*, *48*(1), 34–43. https://doi.org/10.1016/j.coldregions.2006.09.008

Wischmeier, W. H., & Smith, D. D. (1978). *Predicting rainfall erosion losses-a guide to conservation planning*. Hyattsville, MD: USDA, Science and Education Administration.

Xu, J. R., Morris, P. J., Liu, J. G., & Holden, J. (2018). PEATMAP: Refining estimates of global peatland distribution based on a meta-analysis. *Catena*, *160*, 134–140. https://doi.org/10.1016/j.catena.2017.09.010

Yu, Z. C. (2012). Northern peatland carbon stocks and dynamics: A review. *Biogeosciences*, *9*(10), 4071–4085. https://doi.org/10.5194/bg-9-4071-2012